BosonSampling with Non-Simultaneous Photons

Barry C. Sanders

Friday 3 April 2014

Alberta Innovates Technology Futures
CIFAR CANADIAN INSTITUTE for ADVANCED RESEARCH
NSERC CRSNG
Recruitment Program of Global Experts
University of Calgary
University of Waterloo
中国科学技术大学 University of Science and Technology of China

Table of contents

Our Work

- Tan Gao de_Guise BCS "SU(3) Quantum Interferometry with Single-Photon Input Pulses" *PRL* **110** (11) 113603 (2013)
- de_Guise Tan Poulin BCS "Immanants for three-channel linear optical networks" arXiv.org:1402.2391
- Tillmann Tan Stoeckl BCS de_Guise Heilmann Nolte Szameit Walther "BosonSampling with Controllable Distinguishability" arXiv:1403.3433

Aim of Q Computing

Aim: Transform certain C hard computational problems into easy-to-solve Q problems.

- Achieved by exploiting the resources of Q computation
- Unfortunately onerous space & time resources are needed to solve instances beyond current C computational capability.
- One objective is to solve the first computational problem that can be solved with Q but not C computing.
- Sampling problems provide this opportunity.

Motivation

Test the Extended Church-Turing Thesis

Thesis: Any function that is algorithmically computable efficiently can be efficiently computed by a standard (non-$\mathbb{Q}$) model such as a Turing machine.

Falsification occurs if a $\mathbb{Q}$ computer, even a problem-specific purpose-built system such as photon interferometery that eschews $\mathbb{Q}$ bits and $\mathbb{Q}$ gates, solves a computational problem efficiently in a case where classical computing is believed not to solve the same problem efficiently.

Sampling Paradigm: Random Walk

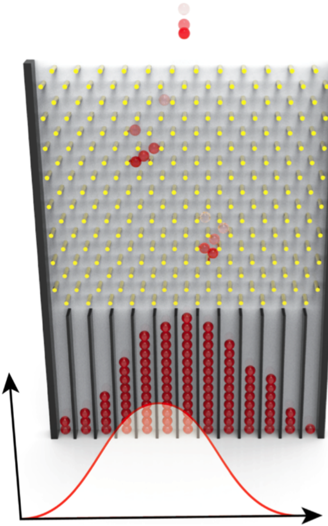

- Quincunx, or Galton Board, samples binomial distribution.
- Demonstrates classical walk.
- Error in sampling the distribution is the 1-norm distance between ideal and measured distribution.
- Algorithmic applications as random-walk oracle.

BosonSampling Problem

Paradigm: Seek efficient Q sampling of C hard-to-sample distribution.

Task: Given random U transforming n input photons (≤ 1 photon per input port) in $m \in \mathrm{poly}(n)$ modes with n input photons, sample output coincidence distribution.

Def$^{\mathrm{n}}$: Permanent of a matrix: $\mathrm{Per}(A) := \sum_\sigma \Pi_i a_{i\sigma(i)}$.

Effect: Sampling from permanent-weighted sub-matrices of U.

Likely: Approximate C sampling of this distribution is probably hard within 1-norm error $\epsilon \in 1/\mathrm{poly}(n)$ and Haar-random U.

Because: Approximating outcome probabilities requires approximating permanents (#P-hard) of U sub-matrices.

Transition Matrix

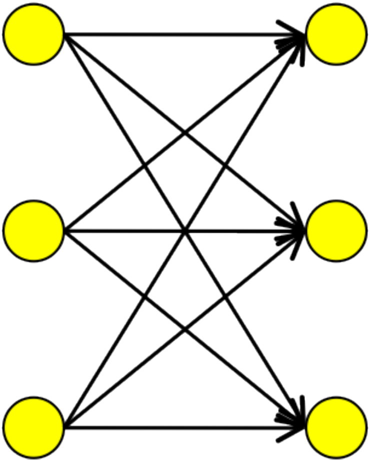

From Aaronson

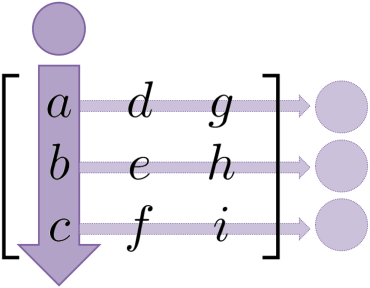

$a, b, c \geq 0$

$a + b + c = 1$

From Arkhipov

Transition Matrix (from Arkhipov)

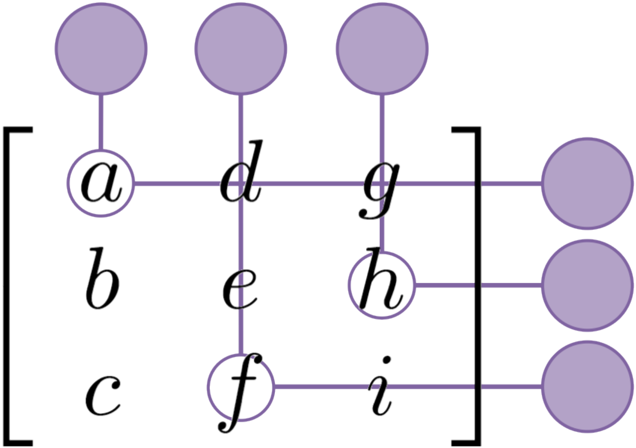

$$\Pr\left[\text{one per slot}\right] = aei + afh$$

Transition Matrix (from Arkhipov)

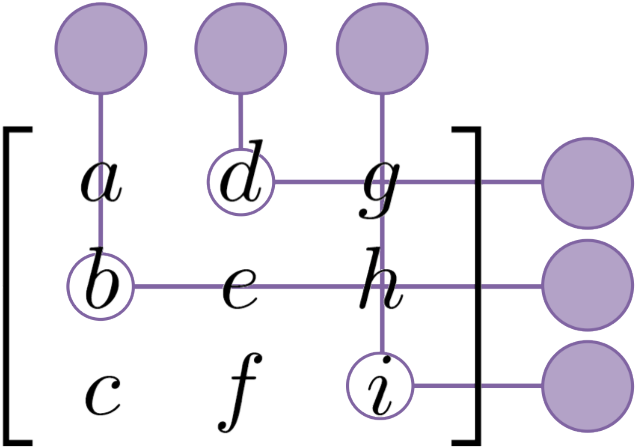

$$\Pr\left[\text{one per slot}\right] = aei + afh + bdi$$

Transition Matrix (from Arkhipov)

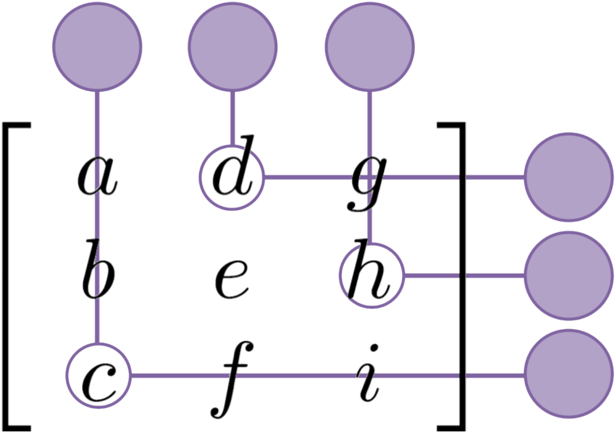

$$\Pr[\text{one per slot}] = aei + afh + bdi + bfg + cdh$$

Transition Matrix (from Arkhipov)

$$\begin{bmatrix} a^2 & d^2 & g^2 & ad & ag & dg \\ b^2 & e^2 & h^2 & be & bh & eh \\ c^2 & f^2 & i^2 & cf & ci & fi \\ 2ab & 2de & 2gh & ae+bd & ah+bg & dh+eg \\ 2ac & 2df & 2gi & af+cd & ai+cg & ei+fh \\ 2bc & 2ef & 2hi & bf+ce & bi+ch & di+fg \end{bmatrix}$$

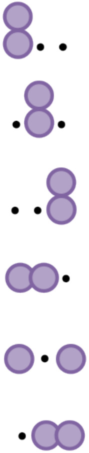

Linear optical interferometer

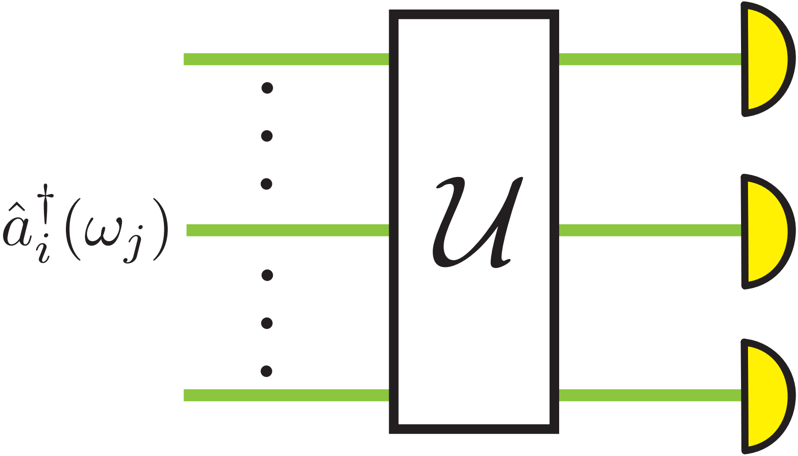

Proving Hardness of the BosonSampling Problem

Strategy: Contrapositive: $\exists$ efficient randomized (NP) algorithm for sampling the boson distribution.

Input: Description of interferometer U with m channels and n photons (≤ 1 entering each port).

Output: Sample from photon distribution with error $< 1/\text{poly}(n)$.

Then: Use output sample for oracle in BPP^{NP} algorithm to estimate (with high probability) $|\text{Per}(A)|^2$ for A a Gaussian matrix.

So: Complexity Polynomial Hierarchy Collapse to third order.

Sketch of Proof

- Embed any $A \in \mathbb{C}^{n\times n}$ in $U = \begin{pmatrix} \epsilon A & B \\ C & D \end{pmatrix} \in \mathbb{C}^{m\times m}$.
- Probability p that state of one photon entering each of first n input ports and zero otherwise yields identical output state scales as $\epsilon^{2n} |\mathrm{Per}(A)|$.
- Estimating $\mathrm{Per}(A)$ is (combinatorially) hard, i.e., #P-complete even for A restricted to entries of 0 and 1 so estimating p implies solving a $\mathrm{P}^{\#P}$ problem.
- Thus, the existence of an efficient randomized algorithm implies $\mathrm{P}^{\#\mathrm{P}} = \mathrm{BPP}^{\mathrm{NP}}$, hence a collapse of the polynomial hierarchy to third order.

NB: Interferometer not solving the permanent itself.

Noise & Error

- $\mathbb{C}$ simulate boson distribution within $\leq 1/\text{poly}(n)$ distance?
- If yes, then AA conjecture a BPP^{NP} algorithm that estimates $|\text{Per}(A)|^2$ with high probability for Gaussian $A \in \mathcal{N}(0,1)_C^{nxn}$.
- Then a noisy n boson experiment falsifies extended Church thesis assuming $\text{P}^{\#\text{P}} \neq \text{BPP}^{\text{N}P}$.
- Relies on conjecture $\Pr\left[\text{Per}(A) \leq e\sqrt{n!}\right] \leq Cn^D e^{\beta}$ for $C, D, \beta > 0$ constants.

AA's Five Obvious Errors in Experimental BosonSampling

1. imperfect preparation of the *n*-photon Fock–state
2. inaccurate description of the interferometer
3. photon losses
4. imperfect detectors
5. non-simultaneity of photon arrival times

Photon losses and imperfect detection ameliorated for demonstrations of principle by post–selection techniques. Inaccuracy of the description of the transition matrix can be minimized by stabilization and process tomography.

Hong-Ou-Mandel dip: Heart of Q Transition Matrix

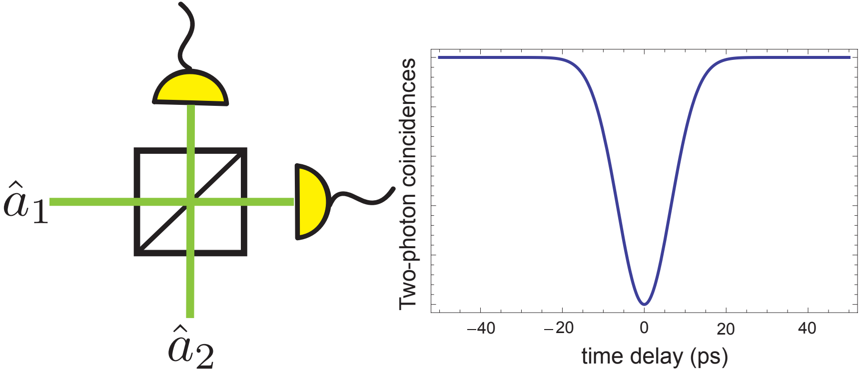

Hong-Ou-Mandel dip

- Importance
  - Characterizes distinguishability between pairs of single photons.
  - Certifies coherence and purity of single photons
- Applications
  - Dense coding and single-qubit fingerprinting
  - Non-deterministic nonlinear gates for optical q computing.
- Beyond
  - Simultaneously characterizing distinguishability between multiple photons.
  - Efficiently sampling immanants of sub matrices of special unitary matrices: $\mathrm{BPP}^{\#\mathrm{P}}$ "the BosonSampling Problem".

Experimental boson sampling: e.g., Walther @ Vienna

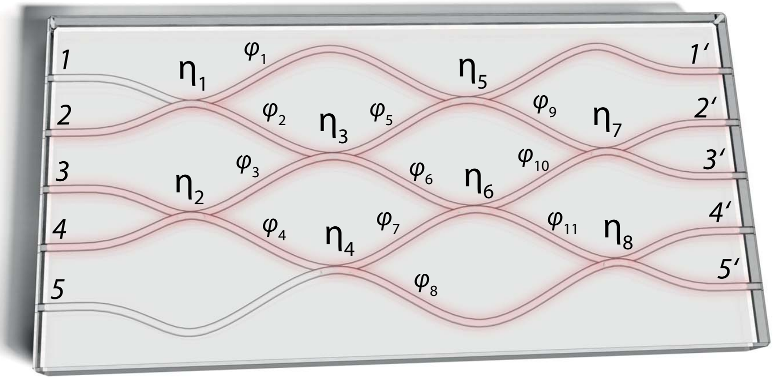

Single photon in a single-mode

- Single photon in a given mode (path) with frequency ω is

$$|1\rangle = \hat{a}^\dagger(\omega)\,|0\rangle\,.$$

- For two path i and j with monochromatic fields of angular frequencies ω_k and ω_l, respectively,

$$\left[\hat{a}_i(\omega_k), \hat{a}_j^\dagger(\omega_l)\right] = \delta_{ij}\delta(\omega_k - \omega_l)\mathbb{1}.$$

- For photon temporal mode $\phi(t)$, the spectral mode is $\mathcal{F}[\phi(t)] = \tilde{\phi}(\omega)$, and single photon in this mode is

$$|1\rangle = \int \mathrm{d}\omega\tilde{\phi}(\omega)\hat{a}^\dagger(\omega)\,|0\rangle\,,\ \int \mathrm{d}\omega\left|\tilde{\phi}(\omega)\right|^2 = 1.$$

Single-photon product states, delays & detections

- Tensor products:

$$|1(\omega_1)\rangle \otimes |1(\omega_2)\rangle =: |1(\omega_1)1(\omega_2)\rangle = \hat{a}_1^\dagger(\omega_1)\hat{a}_2^\dagger(\omega_2)\,|0\rangle\,.$$

- As $\mathcal{F}^{-1}\left[\tilde{\phi}(\omega)\mathrm{e}^{-\mathrm{i}\omega\tau}\right] = \phi(t-\tau)$ a time delay τ effects

$$|1\rangle \mapsto \int \mathrm{d}\omega \tilde{\phi}(\omega)\mathrm{e}^{-\mathrm{i}\omega\tau}|1(\omega)\rangle.$$

- Multi-mode Fock state is

$$|n\rangle := \frac{1}{\sqrt{n!}}\bigotimes_{j=1}^{n}\int \mathrm{d}\omega_j\tilde{\phi}(\omega_j)\hat{a}^\dagger(\omega_j)|0\rangle.$$

Photon Counting

Photon counting projective measure is

$$\Pi_n := |n\rangle\langle n|; \sum_{n=0}^{\infty} \Pi_n = \mathbb{1}.$$

Flat-spectrum incoherent Fock-number state measurement operator:

$$\int \mathrm{d}^n \boldsymbol{\omega} |1(\omega_1)_1 \ldots 1(\omega_n)_n)(1(\omega_1)_1 \cdots 1(\omega_n)_n|.$$

Interferometer transformation

- Action of $\mathcal{U}$ on a single photon entering the i^{th} mode:

$$\hat{\mathbf{a}}^\dagger \mapsto U\hat{\mathbf{a}}^\dagger \longrightarrow \hat{a}_i^\dagger(\omega_j) \mapsto \sum_{k=1}^{n} u_{ki}\hat{a}_k^\dagger(\omega_j).$$

- With one photon per mode over n-mode input,

$$\hat{a}_1^\dagger(\omega_1)\cdots\hat{a}_n^\dagger(\omega_n) \mapsto \sum_{k_1,\cdots k_n}^{n} u_{k_1 1}u_{k_2 2}\cdots u_{k_n 2}\hat{a}_{k_1}^\dagger(\omega_1)\cdots\hat{a}_{k_n}^\dagger(\omega_n).$$

Two-channel interferometry

- Assume passive lossless two-path SU(2) interferometry.
- Irrep basis states are $|\ell m\rangle$ for $\ell \in \{0, \frac{1}{2}, 1, \frac{3}{2}, \dots\}$.
- Smallest faithful representation is $\ell = \frac{1}{2}$:

$$R(\Omega) = \begin{pmatrix} \mathrm{e}^{-i(\alpha+\gamma)} \cos \frac{\beta}{2} & -\mathrm{e}^{-i(\alpha-\gamma)} \sin \frac{\beta}{2} \\ \mathrm{e}^{i(\alpha-\gamma)} \sin \frac{\beta}{2} & \mathrm{e}^{i(\alpha+\gamma)} \cos \frac{\beta}{2} \end{pmatrix}$$

  with Euler angles $\Omega = (\alpha, \beta, \gamma)$.
- Each photon for HOM dip is a spin-$\frac{1}{2}$ particle: one $\uparrow$, one $\downarrow$.

Representation for SU(2) Interferometry

- Young Diagrams for 2 input photons to SU(2) interferometer:

$$\begin{gathered} \square \otimes \square \rightarrow \square\square \oplus \begin{array}{c}\square\\[-4pt]\square\end{array} \\ (1,0) \otimes (1,0) \rightarrow (2,0) \oplus (0,0) \end{gathered} \tag{1}$$

- Two photons of different frequencies are written as a superposition of $|\ell m\rangle$ states

$$|1(\omega_1)1(\omega_2)\rangle = \frac{1}{\sqrt{2}}\left(|0,0\rangle + |1,0\rangle\right),$$

i.e., a superposition of a symmetric and antisymmetric state so only the ω_1 photon is in port 1 and the ω_2 photon is in port 2.

Transformations for SU(2) Interferometry

- $D^{\ell}_{m'm}(\Omega) \equiv \langle \ell m' | R(\Omega) | \ell m \rangle$ are the Wigner D-functions.
- Single-photon transformation under SU(2) interferometry:

$$R(\Omega)\hat{a}_1^\dagger(\omega_1)\,|0\rangle = \left[\hat{a}_1^\dagger(\omega_1) D^{\frac{1}{2}}_{\frac{1}{2},\frac{1}{2}}(\Omega) + \hat{a}_2^\dagger(\omega_1) D^{\frac{1}{2}}_{-\frac{1}{2},\frac{1}{2}}(\Omega)\right]|0\rangle$$

$$R(\Omega)a_2^\dagger(\omega_2)\,|0\rangle = \left[\hat{a}_1^\dagger(\omega_2) D^{\frac{1}{2}}_{\frac{1}{2},-\frac{1}{2}}(\Omega) + a_2^\dagger(\omega_2) D^{\frac{1}{2}}_{-\frac{1}{2},-\frac{1}{2}}(\Omega)\right]|0\rangle\,.$$

- Two-photon transformation as direct sum (singlet+triplet):

$$R(\Omega)|1(\omega_1)1(\omega_2)\rangle = \frac{R(\Omega)\,|0,0\rangle + R(\Omega)\,|1,0\rangle}{\sqrt{2}}.$$

- HOM dip corresponds to vanishing permanent at zero delay:

$$\langle 1,0|R(\Omega)|1(\omega_1)1(\omega_2)\rangle = \frac{1}{\sqrt{2}} D^1_{0,0}(\Omega) = \cos\beta = 0.$$

SU(3)

- Three-mode linear interferometer is described by $SU(3)$ matrix using eight-parameter Euler angles Ω:

$$U = R(\Omega) = R_{23}(\alpha_1, \beta_1, -\alpha_1) R_{12}(\alpha_2, \beta_2, -\alpha_2) \times R_{23}(\alpha_3, \beta_3, -\alpha_3) \mathrm{e}^{-i\gamma_1 h_1} \mathrm{e}^{-i\gamma_2 h_2}$$

for

$$\hat{C}_{ij} = a_i^\dagger \hat{a}_j, \hat{h}_1 = 2\hat{C}_{11} - \hat{C}_{22} - \hat{C}_{33},\ \hat{h}_2 = \frac{1}{2}\left(C_{22} - \hat{C}_{33}\right).$$

- R_{23} and R_{12} are SU(2) operations in the respective subspaces.

Representations for $SU(3)$ Interferometry

- Basis states for irrep (λ, μ) are $|(\lambda, \mu)\nu_1\nu_2\nu_3; I\rangle$ for ν_i the photon # in the i^{th} mode & $\nu_1 + \nu_2 + \nu_3 = \lambda + 2\mu$.
- Young diagram for three-photon case:

$$\begin{gathered}\square \otimes \square \otimes \square \rightarrow \ydiagram{3} \oplus \ydiagram{2,1} \oplus \ydiagram{2,1} \oplus \ydiagram{1,1,1} \\ (1,0) \otimes (1,0) \otimes (1,0) \rightarrow (3,0) \oplus (1,1) \oplus (1,1) \oplus (0,0)\end{gathered} \tag{2}$$

- I distinguishes states of equal weight $(\nu_1 - \nu_2, \nu_2 - \nu_3)$ belonging to different irreps of $SU(2)_{23}$ subgroup.

Immanants of a Matrix

- Immanant generalizes determinant & permanent of a matrix.
- For $\lambda = (\lambda_1, \lambda_2, \lambda_3, \ldots)$ a partition of n & χ_λ the irreducible character of the symmetry group S_n, the immanant of the $n \times n$ matrix $\mathcal{U} = (u_{ij})$ associated with χ_λ is

$$\mathrm{Imm}_\lambda(\mathcal{U}) = \sum_{\sigma \in S_n} \chi_\lambda(\sigma) u_{1\sigma(1)} u_{2\sigma(2)} \ldots u_{n\sigma(n)}$$

- Special cases:

$$\begin{aligned} \chi_\lambda(\sigma) =& \mathrm{sgn}(\sigma) \implies \mathrm{Imm}_\lambda = \mathrm{Det}(\mathcal{U}), \\ \chi_\lambda(\sigma) =& 1 \implies \mathrm{Imm}_\lambda = \mathrm{Per}(\mathcal{U}). \end{aligned}$$

Three Monochromatic Photons

- For three photons in three modes,

$$\begin{aligned}|1(\omega_1)1(\omega_2)1(\omega_3)\rangle &= \frac{1}{\sqrt{6}}\,|(00)000;0\rangle + \frac{1}{\sqrt{6}}\,|(30)111;1\rangle \\ &+\frac{1}{2}\,|(11)111;0\rangle_1 + \frac{1}{\sqrt{12}}\,|(11)111;1\rangle_1 \\ &-\frac{1}{\sqrt{12}}\,|(11)111;0\rangle_2 + \frac{1}{2}\,|(11)111;1\rangle_2\end{aligned}$$

- The overlap in the integral is

$$\begin{aligned}&\langle 1(\omega_1)1(\omega_2)1(\omega_3)|R(\omega)|1(\omega_1)1(\omega_2)1(\omega_3)\rangle \\ &= \frac{1}{6}\mathrm{Per}(R(\Omega)) + \frac{1}{3}\mathrm{Imm}(R(\Omega)) + \frac{1}{6}\mathrm{Det}(R(\Omega))\rangle\end{aligned}$$

Three-fold Photon Coincidences

- The proof relies on the following observations:

$$\begin{aligned}
\mathrm{Per}(R(\Omega)) =& D^{(3,0)}_{(111)1;(111)1}(\Omega) \\
\mathrm{Imm}(R(\Omega)) =& D^{(1,1)}_{(111)1;(111)1}(\Omega) + D^{(1,1)}_{(111)0;(111)0}(\Omega) \\
\mathrm{Det}(R(\Omega)) =& D^{(0,0)}_{(000)0;(000)0}(\Omega)
\end{aligned}$$

- Then using the definition of the $SU(3)$ Wigner D-function,

$$D^{(\lambda,\mu)}_{(111)J,(111)I}(\Omega) = \langle(\lambda,\mu)(111)J|R(\Omega)|(\lambda,\mu)(111)I\rangle \tag{3}$$

and the decomposition of $|1(\omega_1)1(\omega_2)1(\omega_3)\rangle$ in the coupled irrep basis, we can work out the relationship.

The coincidence rate of each landscape corresponds to

$$P_{111}(\Delta\tau_1, \Delta\tau_2) = \int d\omega \int d\omega' \int d\omega'' |\langle\psi_{\text{in}}| \hat{M}^\dagger \hat{a}_1^\dagger(\omega)\hat{a}_2^\dagger(\omega')\hat{a}_3^\dagger(\omega'')|0\rangle|^2$$

$$= \mathbf{v}^\dagger \Big[\mathbb{1} + \varrho_{12}\zeta_{12}\mathrm{e}^{-\xi_{12}\Delta\tau_1^2} + \varrho_{23}\zeta_{23}\mathrm{e}^{-\xi_{23}\Delta\tau_2^2}$$

$$+ \varrho_{13}\zeta_{13}\mathrm{e}^{-\xi_{13}(\Delta\tau_1 - \Delta\tau_2)^2}$$

$$+ \varrho_{123}\zeta_{123}\left(\mathrm{e}^{-\xi_{123}(\Delta\tau_1, \Delta\tau_2)} + \mathrm{e}^{-\xi^*_{123}(\Delta\tau_1, \Delta\tau_2)}\right)\Big]\mathbf{v}$$

with $\hat{M}$ a 3×3 transformation submatrix.

$$\mathbf{v} := \begin{pmatrix} \mathrm{per}(M) \\ \det(M) \\ \frac{1}{2\sqrt{3}}\mathrm{Imm}(M) + \frac{1}{2\sqrt{3}}\mathrm{Imm}(M_{312}) \\ \frac{1}{6}\mathrm{Imm}(M) - \frac{1}{3}\mathrm{Imm}(M_{132}) - \frac{1}{6}\mathrm{Imm}(M_{213}) + \frac{1}{3}\mathrm{Imm}(M_{312}) \\ \frac{1}{6}\mathrm{Imm}(M) + \frac{1}{3}\mathrm{Imm}(M_{132}) + \frac{1}{6}\mathrm{Imm}(M_{213}) + \frac{1}{3}\mathrm{Imm}(M_{312}) \\ -\frac{1}{2\sqrt{3}}\mathrm{Imm}(M) + \frac{1}{2\sqrt{3}}\mathrm{Imm}(M_{213}) \end{pmatrix}$$

with M_{ijk} a permuted M such that its rows are arranged in order i, j and k.

Sample Theoretical Plots for Three-Photon Coincidences

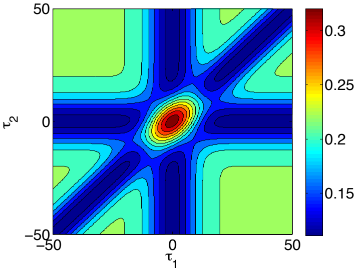

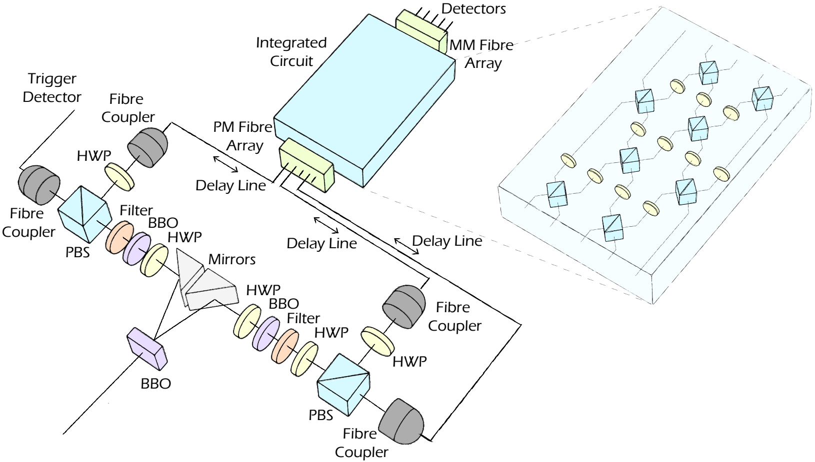
Detectors
Integrated Circuit
MM Fibre Array
Trigger Detector
Fibre Coupler
HWP
PM Fibre Array
Delay Line
Fibre Coupler
Filter
BBO
HWP
PBS
Mirrors
Delay Line
Delay Line
HWP
BBO
Filter
HWP
Fibre Coupler
HWP
BBO
PBS
Fibre Coupler

- Cases: 3 photons enter $\{1, 2, 4\}$, exit $\{1, 3, 4\}$ or $\{3, 4, 5\}$.
- Intersections of (input) columns and (output) rows select 3×3 sub-matrices.
- Tune temporal delays $\Delta\tau_1$ and $\Delta\tau_2$ & sample 6 pts.
- Theoretical prediction (left bars).
- Experimentally obtained output probabilities (right bars)
- χ^2_{red} is 1.38 and 1.10 respectively.

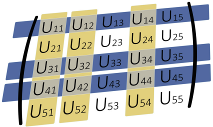
U11 U12 U13 U14 U15
U21 U22 U23 U24 U25
U31 U32 U33 U34 U35
U41 U42 U43 U44 U45
U51 U52 U53 U54 U55

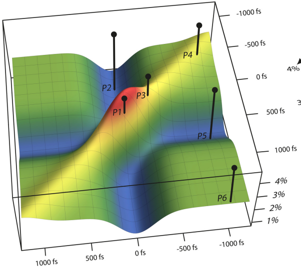
-1000 fs
-500 fs
0 fs
500 fs
1000 fs
4%
3%
2%
1%
1000 fs
500 fs
0 fs
-500 fs
-1000 fs
P1
P2
P3
P4
P5
P6

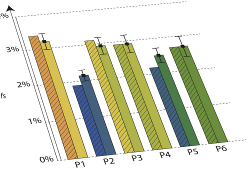
4%
3%
2%
1%
0%
P1
P2
P3
P4
P5
P6

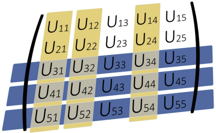
U11 U12 U13 U14 U15
U21 U22 U23 U24 U25
U31 U32 U33 U34 U35
U41 U42 U43 U44 U45
U51 U52 U53 U54 U55

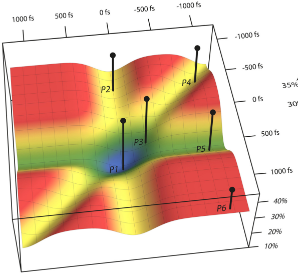
1000 fs
500 fs
0 fs
-500 fs
-1000 fs
-1000 fs
-500 fs
0 fs
500 fs
1000 fs
40%
30%
20%
10%
P1
P2
P3
P4
P5
P6

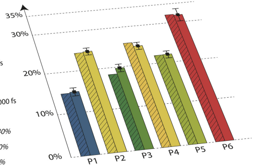
35%
30%
20%
10%
0%
P1
P2
P3
P4
P5
P6

State generation

- 80 MHz Ti–Sapphire oscillator
  - 150 fs pulses
  - 789 nm
  - Rep rate of 80 MHz
- Frequency doubled in a LiB_3O_5 (LBO) crystal.
- SHG output power controlled by a power regulation stage comprising HWP and PBS placed before the LBO-crystal.
- Resulting emission at 394.5 nm is focused into a 2 mm thick β–BaB_2O_4 (BBO) crystal cut for degenerate non-collinear type-II down-conversion.

Compensation and Fibre Coupling

- Comprises HWPs and 1 mm thick BBO–crystals for countering temporal and spatial walk–off.
- The two spatial outputs of the down–converter
  - pass through narrowband ($\lambda_{\mathsf{FWHM}} = 3$ nm) interference filters
  - achieve a coherence time greater than the birefringent walk–off due to group velocity mismatch in the crystal.
  - renders the photons close to spectral indistinguishability
  - aligned to emit $|\phi^+\rangle = \frac{1}{\sqrt{2}}(|HH\rangle + |VV\rangle)$ when pumped at 205 mW cw–equivalent pump power.
- The state is coupled into single-mode fibers (Nufern 780–HP) equipped with pedal–based polarization controllers to counter any stress–induced rotation of the polarization inside the fiber.

Fibres

- Each spatial modes coupled to one input of a PBS with other input in a vacuum.
- Outputs pass HWPs then coupled to 4 polarization-maintaining fibers (Nufern PM780–HP).
- Temporal overlap controlled by 2 motorized delay lines that exhibit a bidirectional repeatability of ± 1 μm.
- Temporal alignment precision $\approx \pm 5$ μm.
- Precision limit 5% of photon coherence length.
- Polarization-maintaining fibers mated to single-mode fiber v–groove–array (Nufern PM780–HP) with a pitch of 127 μm and butt–coupled to the integrated circuit.
- Coupling controlled by a manual six-axis flexure stage and stable within 5% of total single–photon counts over 12 hours.
- Output fiber array is a multimode v–groove–array (GIF–625).

Detection

- Single-photon avalanche photodiodes
- Recorded with FPGA logic.
- Coincidence time window was set to 3 ns.
- BBO was pumped with cw-equivalent power of 700 mW
- Ratio of six–photon emission vs desired four–photon emission was $< 5\%$.

Integrated network fabrication.

- Fabricated using a fs-direct-laser-writing technique.
- Laser pulses were focused 370 μm under the surface of a high–purity fused silica sample by a $NA = 0.6$ objective.
- 200 nJ pulses exhibit pulse duration of 150 fs at 100 kHz repetition rate and central wavelength of 800 nm.
- To write guiding modes the probe was translated at 6 cm/min.
- Modes show a field diameter of 21.4 μm$\times$17.2 μm for $\lambda = 789$ nm and propagation loss of 0.3 dB/cm.
- Coupling loss of -3.5 dB.
- Coupling to output array results in negligible loss due to use of multimode fibers.